COMMUNICATIONS IN APPLIED NUMERICAL METHODS, Vol. 8, 497–504 (1992)

PLATE QUADRILATERAL FINITE ELEMENT WITH INCOMPATIBLE MODES*

ADNAN IBRAHIMBEGOVIĆ
Swiss Federal Institute of Technology, LSC, GC, A2, CH-1015, Lausanne, Switzerland

SUMMARY

A four-node quadrilateral plate element with a set of incompatible modes is presented in this work. In an analysis of thin plates, the element exhibits a similar performance as the well known discrete Kirchhoff plate element. The computational effort associated with the element is also comparable to that associated with the discrete Kirchhoff element. However, as opposed to the discrete Kirchhoff plate element, the presented plate element is based on the Reissner–Mindlin plate theory and can be used in a thick plate analysis as well.

INTRODUCTION

A couple of new quadrilateral plate elements have been presented recently in Reference 1. The elements are based on Reissner[2]–Mindlin[3] plate theory, a hierarchical displacement interpolation and an assumed shear strain field.[4] We have also demonstrated[1] how the well known discrete Kirchhoff plate element[5] fits consistently within the proposed framework.

The quadrilateral thick plate element proposed in Reference 1, which is equivalent to the discrete Kirchhoff quadrilateral, has in total 16 degrees of freedom: 12 nodal degrees of freedom and 4 edge degrees of freedom (normal mid-side rotations). Introducing edge degrees of freedom may be desirable to facilitate easier construction of a complete interpolation polynomial, which has proven to have superior accuracy in many applications (e.g. see Reference 6). However, the presence of the edge degrees of freedom is somewhat undesirable from the standpoint of a standard computer program architecture, which normally carries degrees of freedom associated with the nodal points only.

Therefore, on the basis of the thick element[1] with 12 nodal and four edge degrees of freedom, we construct an element with degrees of freedom associated with the nodal points only. In that process, the mid-side normal rotations are identified as the incompatible modes[7] interpolation parameters, and via use of the static condensation procedure[8] they are eliminated at the element level. It is shown in this work that such an element still keeps all the desirable properties of its compatible predecessor. The successful addition of incompatible modes is performed by following the methodology proposed in the work of Ibrahimbegović and Wilson.[9]

The element presented can be used as an equivalent to the discrete Kirchhoff plate element in a thin plate analysis. However, as opposed to the discrete Kirchhoff, this element can also be applied in analysis of thick plates.

* Dedicated to Professor Edward L. Wilson on the occasion of his retirement.

0748–8025/92/080497–08$09.00

Received 12 June 1991
Revised 29 October 1991

The triangular plate element can be obtained by degenerating the proposed quadrilateral, as it was done with the discrete Kirchhoff element in Reference 10.

REISSNER–MINDLIN PLATE THEORY

The variational formulation for the Reissner–Mindlin plate theory is given by (e.g. see Reference 11)

$$\mathrm{DII}(\omega, \theta_i)(\hat{\omega}, \hat{\theta}_i) = \int_\Omega \hat{\varkappa}_{ij}(\hat{\theta}_i) C^{\mathrm{B}}_{ijkl} \varkappa_{kl}(\theta_i)\, \mathrm{d}\Omega + \int_\Omega \hat{\gamma}_i(\hat{\omega}, \hat{\theta}_i) C^{\mathrm{S}}_{ij} \gamma_j(\omega, \theta_i)\, \mathrm{d}\Omega$$

$$- \int_\Omega \hat{\omega} f\, \mathrm{d}\Omega = 0, \qquad i, j, k, l \in \{1, 2\} \tag{1}$$

where the curvature tensor $\varkappa_{ij}$ is related to the director rotation β_i via

$$\varkappa_{ij} = \frac{1}{2}\left(\frac{\partial \beta_i}{\partial x_j} + \frac{\partial \beta_j}{\partial x_i}\right) \tag{2}$$

and the director rotation is related to the right-hand-rule rotation vector θ_i via an alternating tensor e_{ij}

$$\beta_i = e_{ij}\theta_j, \qquad e_{ij} = \begin{bmatrix} 0 & -1 \\ +1 & 0 \end{bmatrix} \tag{3}$$

In (1), γ_i are shear strain components

$$\gamma_i = \frac{\partial \omega}{\partial x_i} - \beta_i \tag{4}$$

For simplicity, in (1) we assumed linear elastic constitutive equations and the Dirichlet boundary value problem with the homogeneous boundary conditions. However, the discussion to follow applies to more general constitutive equations and other kinds of boundary conditions as well.

The discrete formulation which corresponds to (1) is

$$\mathrm{DII}(\omega^h, \theta^h) \cdot (\hat{\omega}^h, \hat{\theta}^h) = \int_{\Omega^h} \hat{\boldsymbol{\varkappa}}^{h\mathrm{T}} \mathbf{C}^{\mathrm{B}} \boldsymbol{\varkappa}^h\, \mathrm{d}\Omega + \int_{\Omega^h} \hat{\boldsymbol{\gamma}}^{h\mathrm{T}} \mathbf{C}^{\mathrm{S}} \boldsymbol{\gamma}^h\, \mathrm{d}\Omega - \int_{\Omega^h} \hat{\omega}^h f\, \mathrm{d}\Omega = 0 \tag{5}$$

The mapping of generalized strain measures which is introduced in the discrete formulation (5), i.e.

$$\varkappa_{ij} \mapsto \boldsymbol{\varkappa}^h = \langle -\partial\theta_2/\partial x_1,\ \partial\theta_1/\partial x_2,\ \partial\theta_1/\partial x_1 - \partial\theta_2/\partial x_2 \rangle^{\mathrm{T}} \tag{6}$$

and

$$\gamma_i \mapsto \boldsymbol{\gamma}^h = \langle \gamma_1, \gamma_2 \rangle^{\mathrm{T}} \tag{7}$$

determines the form of the constitutive matrices $\mathbf{C}^{\mathrm{B}}$ and $\mathbf{C}^{\mathrm{S}}$. For example, in the case of an isotropic linear elastic plate,

$$\mathbf{C}^{\mathrm{B}} = \frac{Et^3}{12(1-\nu^2)} \begin{bmatrix} 1 & \nu & 0 \\ \nu & 1 & 0 \\ 0 & 0 & 1-\nu/2 \end{bmatrix}, \quad \mathbf{C}^{\mathrm{S}} = \frac{Etc}{2(1+\nu)} \begin{bmatrix} 1 & 0 \\ 0 & 1 \end{bmatrix} \tag{8}$$

where t is the plate thickness, E is Young's modulus and ν is Poisson's ratio. The shear correction factor c is usually set to 5/6.

Superscript h in (5) is the mesh parameter which is used to denote the quantities in the discrete approximation.

FINITE-ELEMENT INTERPOLATION

We consider a four-node quadrilateral plate element in Figure 1. The reference configuration of the element is defined by the bilinear mapping

$$\mathbf{x}^h \mid_{\Omega^e} = \mathbf{x}^e = \sum_{I=1}^{4} N_I(r, s)\mathbf{x}_I \tag{9}$$

where $\mathbf{x}^e = \langle x_1; x_2 \rangle^T$ is the vector of local co-ordinates, $\mathbf{x}_I$ are the nodal values of that vector, and $N_I(r, s)$ are standard bilinear shape functions (e.g. see Reference 12),

$$N_I(r, s) = \tfrac{1}{4}(1 + r_I r)(1 + s_I s), \quad I = 1, 2, 3, 4 \tag{10}$$

Natural co-ordinates (r, s) are defined on interval $\{-1, 1\}$.

The curvature vector $\boldsymbol{\varkappa}^e$ is determined by superposing the compatible and incompatible contribution as

$$\boldsymbol{\varkappa}^h \mid_{\Omega^e} = \boldsymbol{\varkappa}_e = \sum_{I=1}^{4} \mathbf{B}_I(r, s)\boldsymbol{\theta}_I + \sum_{L=5}^{8} \hat{\mathbf{B}}_L(r, s)\mathbf{n}_{JK}\alpha_L^e, \quad \boldsymbol{\theta}_I = \begin{pmatrix} \theta_{1I} \\ \theta_{2I} \end{pmatrix} \tag{11}$$

where $\mathbf{B}_I$ has the form

$$\mathbf{B}_I(r, s) = \begin{bmatrix} 0 & -\partial N_I(r, s)/\partial x_1 \\ \partial N_I(r, s)/\partial x_2 & 0 \\ \partial N_I(r, s)/\partial x_1 & -\partial N_I(r, s)/\partial x_2 \end{bmatrix} \tag{12}$$

The outward unit normal vector $\mathbf{n}_{JK}$ for the plate element edge between corner nodes J and K (see Figure 1) is given by

$$\mathbf{n}_{JK} = \begin{pmatrix} \cos \phi_{JK} \\ \sin \phi_{JK} \end{pmatrix} \tag{13}$$

where the corner nodes J and K can be defined by a FORTRAN-like expression

$$L = 5, 6, 7, 8, \qquad J = L - 4, \qquad K = \mathrm{mod}(L, 4) + 1 \tag{14}$$

The strain-displacement matrix $\mathbf{B}_L(r, s)$, $L = 5, 6, 7, 8$, has the same form as the matrix $\mathbf{B}_I$

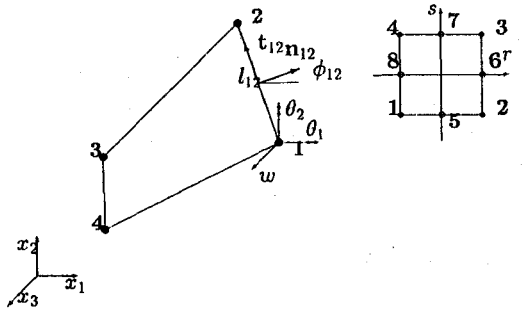

Figure 1. Plate element

in (12), but the serendipity shape functions[12] are used instead of the bilinear ones, where

$$N_L(r,s) = \tfrac{1}{2}(1-r^2)(1+s_L s), \qquad L = 5,7 \tag{15}$$

$$N_L(r,s) = \tfrac{1}{2}(1-s^2)(1+r_L r), \qquad L = 6,8 \tag{16}$$

The strain-displacement matrix $\hat{\mathbf{B}}_L(r,s)$ in equation (11) is produced by purifying $\mathbf{B}_L$ of constant curvature states, in order to satisfy the patch test[13] requirements. Namely, we use the modification[9]

$$\hat{\mathbf{B}}_L(r,s) = \mathbf{B}_L(r,s) - \frac{1}{\Omega^e}\int_{\Omega^e} \mathbf{B}_L(r,s)\,\mathrm{d}\Omega \tag{17}$$

In equation (11), α_L^e, $L = 5,6,7,8$, are incompatible mode interpolation parameters, which correspond to the mid-side hierarchical rotations. Namely, the curvature-rotation matrix in (11) is consistent with a hierarchical rotation interpolation

$$\boldsymbol{\theta}^h|_{\Omega^e} = \boldsymbol{\theta}^e = \sum_{I=1}^{4} N_I(r,s)\boldsymbol{\theta}_I + \sum_{L=5}^{8} N_L(r,s)\mathbf{n}_{JK}\alpha_L^e \tag{18}$$

The assumed shear strain field is bilinear over an element, i.e.

$$\boldsymbol{\gamma}|_{\Omega^e} = \boldsymbol{\gamma}_e \sum_{I=1}^{4} N_I(r,s)\boldsymbol{\gamma}_I + \sum_{I=1}^{4} N_I(r,s)\frac{2}{3\mathbf{t}_{IJ}^{\mathrm{T}}\mathbf{n}_{IK}}\left[\mathbf{n}_{IJ}\alpha_M^e - \mathbf{n}_{IK}\alpha^e{}_L\right] \tag{19}$$

where nodal parameters $\boldsymbol{\gamma}_I$ are computed to be consistent with the constant shear strain distribution along each edge. For a typical node I we get

$$\boldsymbol{\gamma}_I = \frac{1}{\mathbf{t}_{IJ}^{\mathrm{T}}\mathbf{n}_{IK}}\left[\frac{1}{l_{IK}}\mathbf{n}_{IJ}\omega_K + \frac{1}{l_{IJ}}\mathbf{n}_{IK}\omega_J - \left(\frac{1}{l_{IK}}\mathbf{n}_{IJ} + \frac{1}{l_{IJ}}\mathbf{n}_{IK}\right)\omega_I \right.$$

$$\left. + \tfrac{1}{2}\mathbf{n}_{IJ}\mathbf{n}_{IK}^{\mathrm{T}}\boldsymbol{\theta}_K - \tfrac{1}{2}\mathbf{n}_{IK}\mathbf{n}_{IJ}^{\mathrm{T}}\boldsymbol{\theta}_J + \tfrac{1}{2}(\mathbf{n}_{IJ}\mathbf{n}_{IK}^{\mathrm{T}} - \mathbf{n}_{IK}\mathbf{n}_{IJ}^{\mathrm{T}})\boldsymbol{\theta}_I\right] \tag{20}$$

In equations (19) and (20), indices are defined by

$$I = 1,2,3,4, \quad J = \mathrm{mod}(I,4)+1, \quad K = I-1+4*\mathrm{int}(1/I), \quad L = K+4, \quad M = I+4 \tag{21}$$

and l_{IJ} is the length of the plate element edge between corner nodes I and J (see Figure 1), i.e.

$$l_{IJ} = ((x_{I1}-x_{J1})^2 + (x_{I2}-x_{J2})^2)^{(1/2)} \tag{22}$$

The detailed derivation of equation (20) is given in Reference 1.

Having defined the curvature (11) and the shear strain in interpolation (19), we can compute the element stiffness matrix from the equation (5). It is initially of the size 16×16. After the static condensation is performed to eliminate four incompatible mode parameters $\boldsymbol{\alpha}^e$, we obtain the 12×12 stiffness matrix.

In the basic variational structure of the incompatible mode formulation,[9] there are no element loads associated with the incompatible mode parameters. For simplicity, we can use the bilinear interpolation (lumped form) for the loading vector, defined by

$$\mathbf{f}_I = \int_{\Omega^e} N_I(r,s) f\,\mathrm{d}\Omega, \qquad I = 1,2,3,4 \tag{23}$$

NUMERICAL EXAMPLES

Several numerical examples are solved using the plate element presented herein. In the results to follow the plate element is denoted as PQI.

All numerical computations are performed by using 2×2 Gauss quadrature (e.g. see Reference 12). The bending moments are first computed at the Gauss quadrature points to obtain their optimal accuracy.[14] They are then projected to the nodes by using the least-squares fit over an element to the bilinear smoothed field.[12]

Patch test

First, we have checked that the plate element PQI passes the patch test.[13] For that purpose, a square patch of distorted elements is subjected first to pure bending and then to pure twist.

Uniform loading on simply supported square plate

The test problem of a simply supported square plate under uniform loading (see Figure 2) is used to compare our element with the discrete Kirchhoff plate element.[5] The plate is made of linear elastic isotropic material, with Young's modulus $E = 10{\cdot}92$ and Poisson's ratio

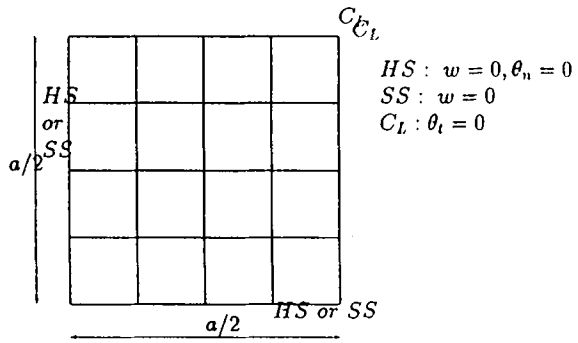

Figure 2. Uniform loading on simply supported square plate

Table I. Uniform loading on thin square plate

Result	Centre displacement				Centre moment			
Support	Hard		Soft		Hard		Soft	
Mesh/elem·	PQI	DKQ	PQI	DKQ	PQI	DKQ	PQI	DKQ
1×1	46026	37847	48708	37903	8·129	6·031	8·959	6·126
2×2	42512	40456	44613	40458	5·597	5·010	5·659	5·006
4×4	41115	40600	42273	40600	4·979	4·839	5·081	4·839
8×8	40761	40619	41395	40619	4·836	4·801	4·892	4·801
16×16	40673	40622	41060	40622	4·800	4·792	4·835	4·792
32×32	40651	40623	40961	40623	4·792	4·789	4·819	4·789
'exact'	40644	40644	—	—	4·793	4·793	—	—

Table II. Uniform loading on thick square plate

Result	Centre displacement				Centre moment			
Support	Hard		Soft		Hard		Soft	
Mesh/elem.	PQI	DKQ	PQI	DKQ	PQI	DKQ	PQI	DKQ
1 × 1	48·682	37·847	51·687	37·903	8·115	6·031	8·914	6·126
2 × 2	44·709	40·456	47·743	40·458	5·591	5·010	5·808	5·006
4 ×	43·225	40·600	46·122	40·600	4·979	4·839	5·238	4·839
8 × 8	42·852	40·619	46·002	40·619	4·836	4·801	5·117	4·801
16 × 16	42·759	40·622	46·103	40·622	4·800	4·792	5·099	4·792
32 × 32	42·736	40·623	46·150	40·623	4·792	4·789	5·096	4·789
'exact'	42·728	42·728	—	—	4·793	4·793	—	—

$\nu = 0{\cdot}3$. The side length $a = 10$ and two values for the plate thickness $t = 0{\cdot}1$ (thin plate) and $t = 1$ (thick plate) are selected. Analytical solution for the thin plate is given in Reference 15, and it can be corrected to account for shear deformation to get the solution for the thick plate.

Both so-called hard ($\omega = 0$ and $\theta_n = 0$) and soft ($\omega = 0$) simply supported boundary conditions are used. In the element PQI, representation of the hard simple support boundary condition is disturbed by inability to set the corresponding incompatible modes equal to zero (recall that they can be identified with hierarchical mid-side rotations). However, this does not influence significantly the accuracy of the computed results.

The numerical results are obtained by modelling one quadrant of the plate using uniform finite-element meshes (see Figure 2). The results are presented in Table I for the thin plate and in Table II for the thick plate along with the results obtained by the discrete Kirchhoff element.

Considering the results in Table I, we can state that the overall convergence rates for elements PQI and DKQ appear to be similar.

The results presented in Table II, showing convergence in centre displacement and centre bending moment, indicate that PQI can be used successfully in an analysis of thick plates. The discrete Kirchhoff element, however, is naturally converging again to the 'thin plate solution', thus introducing significant errors in the computed quantities.

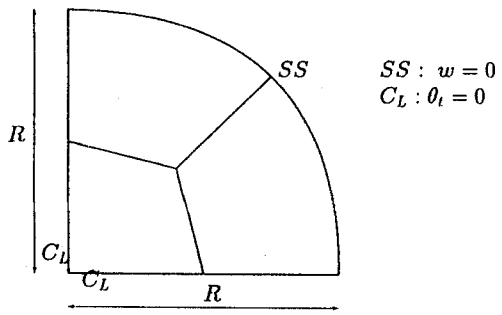

Figure 3. Uniform loading on simply supported circular plate

Uniform loading on simply supported circular plate

The test problem of a uniform loading on the simply supported circular plate is used to illustrate performance of the plate element PQI in an arbitrarily distorted element configuration. The original method of incompatible modes[7] did not converge in such a case.

The computations are performed on a quarter of circular plate of radius $R = 5$ (see Figure 3), using the same properties as in the previous example ($E = 10{\cdot}92$, $\nu = 0{\cdot}3$, $t = 0{\cdot}1$ and 1, and $q = 1$). The accuracy of the results, which are reported in Table III, show that the presented plate element, based on the modified method of incompatible modes,[9] faces no difficulties in an arbitrarily distorted element configuration.

Table III. Uniform loading on circular plate

Result	Centre displacement		Centre bending moment	
No. elem./thick.	$t = 1$	$t = 0{\cdot}1$	$t = 1$	$t = 0{\cdot}1$
3	41·029	39293·	5·209	5·233
12	41·544	39775·	5·178	5·180
48	41·608	39841·	5·159	5·158
192	41·610	39842·	5·157	5·157
'exact'	41·599	39832	5·156	5·156

CLOSURE

The paper presents a method which allows shearing deformations to be incorporated into the standard DKQ and DKT plate bending formulations.

In constructing the finite-element interpolation scheme for the plate element PQI, presented herein, a fundamental role is played by the assumed shear strain interpolation and a set of incompatible modes used to enrich the bending strain interpolation. In order to provide a satisfying performance of the method of incompatible modes, we rely on the methodology presented in collaboration with Ed Wilson.[9]

The plate element PQI shares with the DKQ the same number of degrees of freedom (incompatible modes are eliminated at the element level) and the same accuracy in an analysis of very thin plates. However, as opposed to the DKQ element, the element PQI can also be used successfully in an analysis of thick plates.

ACKNOWLEDGEMENTS

This work was supported by the Swiss National Science Foundation, grant no. 21-28942.90. The help of Mr B. Rebora in performing numerical computations is appreciated.

REFERENCES

1. A. Ibrahimbegović, 'Quadrilaterial finite elements for analysis of thick and thin plates', LSC Internal Report 91/6, Swiss Federal Institut of Technology, 1991 (submitted to *Comput. Methods Appl. Mech. Eng.*).

2. E. Reissner, 'The effect of transverse shear deformation on the bending of elastic plates', *J. Appl. Mech.*, **12**, 69–76 (1945).
3. R. D. Mindlin, 'Influence of rotatory inertia and shear in flexural motion of isotropic elastic plates', *J. Appl. Mech.*, **18**, 31–38 (1951).
4. T. J. R. Hughes and T. E. Tezduyar, 'Finite elements based upon Mindlin plate theory with particular reference to the four-node bilinear isoparametric element', *J. Appl. Mech.*, **46**, 587–596 (1981).
5. J. L. Batoz and M. B. Tahar, 'Evaluation of a new quadrilateral thin plate bending element', *Int. j. numer. methods eng.*, **18**, 1655–1677 (1982).
6. E. L. Wachspress, 'High order curved finite elments', *Int. j. numer. methods eng.*, **17**, 735–745 (1981).
7. E. L. Wilson, R. L. Taylor, W. P. Doherty and J. Ghaboussi, 'Incompatible displacement models', in *Numerical and Computer Methods in Structural Mechanics*, S. J. Fenves, N. Perrone, A. R. Robinson and W. C. Schnobrich (Eds), Academic Press, 1973, pp. 43–57.
8. E. L. Wilson, 'The static condensation algorithm,' *Int. j. numer. methods eng.*, **8**, 199–203 (1974).
9. A. Ibrahimbegović and E. L. Wilson, 'A modified method of incompatible modes', *Commun. Appl. Numer. Methods*, **7**, 187–194 (1991).
10. A. Ibrahimbegović and E. L. Wilson, 'A unified formulation for triangular and quadrilateral flat shell finite elements with six nodal degrees of freedom', *Commun. Appl. Numer. Methods*, **7**, 1–9 (1991).
11. T. J. R. Hughes, *The Finite Element Method: Linear Static and Dynamic Analysis*, Prentice-Hall, Englewood Cliffs, 1987.
12. O. C. Zienkiewicz and R. L. Taylor, *The Finite Element Method: Basic Formulation and Linear Problems*, Vol. I, McGraw-Hill, London, 1989.
13. R. L. Taylor, J. C. Simo, O. C. Zienkiewicz and A. C. Chan, 'The patch test: a condition for assessing finite element convergence', *Int. j. numer. methods eng.*, **22**, 39–62 (1986).
14. J. Barlow, 'Optimal stress locations in finite elements', *Int. j. numer. methods eng.*, **10**, 243–251 (1976).
15. S. P. Timoshenko and S. Woinowsky-Krieger, *Theory of Plates and Shells*, McGraw-Hill, London, 1959.